Original Article

Mechanical environment for lower canine T-loop retraction compared to en-masse space closure with a power-arm attached to either the canine bracket or the archwire

Feifei Jiang[a]; W. Eugene Roberts[b]; Yanzhi Liu[c]; Abbas Shafiee[c]; Jie Chen[d]

ABSTRACT

Objectives: To assess the mechanical environment for three fixed appliances designed to retract the lower anterior segment.

Materials and Methods: A cone-beam computed tomography scan provided three-dimensional morphology to construct finite element models for three common methods of lower anterior retraction into first premolar extraction spaces: (1) canine retraction with a T-loop, (2) en-masse space closure with the power-arm on the canine bracket (PAB), and (3) power-arm directly attached to the archwire mesial to the canine (PAW). Half of the symmetric mandibular arch was modeled as a linear, isotropic composite material containing five teeth: central incisors (L1), lateral incisor (L2), canine (L3), second premolar (L4), and first molar (L5). Bonded brackets had 0.022-in slots. Archwire and power-arm components were 0.016 × 0.022 in. An initial retraction force of 125 cN was used for all three appliances. Displacements were calculated. Periodontal ligament (PDL) stresses and distributions were calculated for four invariants: maximum principal, minimum principal, von Mises, and dilatational stresses.

Results: The PDL stress distributions for the four invariants corresponded to the displacement patterns for each appliance. T-loop tipped the canine(s) and incisors distally. PAB rotated L3 distal in, intruded L2, and extruded L1. PAW distorted the archwire resulting in L3 extrusion as well as lingual tipping of L1 and L2. Maximum stress levels in the PDL were up to 5× greater for the PAW than the T-loop and PAB methods.

Conclusions: T-loop of this type is more predictable because power-arms can have rotational and archwire distortion effects that result in undesirable paths of tooth movement. (*Angle Orthod.* 2020;90:801–810.)

KEY WORDS: Canine retraction; En-masse retraction; Finite element method; Initial displacement; Stress and strain

INTRODUCTION

Both frictionless segmental wire and sliding mechanics for en-masse anterior segment retraction are used to retract canines or anterior teeth. The T-loop (TL), a type of segmental wire, is used to retract the canines,[1] while the sliding mechanics are used for en-masse anterior segment retraction.[2] These orthodontic forces change the mechanical environment (ME) surrounding

[a] Postdoctoral Fellow, Department of Mechanical and Energy Engineering, Indiana University Purdue University Indianapolis (IUPUI), Indianapolis, Ind.

[b] Professor Emeritus, Department of Orthodontics and Oral Facial Genetics, IU School of Dentistry, IUPUI, Indianapolis, Ind.

[c] Graduate student, Department of Mechanical and Energy Engineering, Indiana University Purdue University Indianapolis (IUPUI), Indianapolis, Ind.

[d] Professor and Chair, Department of Mechanical and Energy Engineering, Professor, Department of Orthodontics and Oral Facial Genetics, Indiana University Purdue University Indianapolis (IUPUI), Indianapolis, Ind.

Corresponding author: Dr Jie Chen, PhD, Department of Mechanical and Energy Engineering, Purdue School of Engineering and Technology, IUPUI, 723 West Michigan Street, Indianapolis, IN 46202, USA
(e-mail: jchen3@iupui.edu)

Accepted: June 2020. Submitted: May 2020.
Published Online: September 9, 2020

the tooth, causing it to move. Although all three methods are used clinically, their effects have not been quantified and compared. To control treatment outcomes, quantifying the load components and the resulting changes in ME are essential.

The stresses of orthodontic force alter the ME of the cells in the periodontal ligament (PDL) and alveolar bone, causing bone modeling and remodeling.[1] The effects on the cells can be categorized by the following components: the first principal stress (P1), called maximum tensile stress if positive, stretches the cells; the third principal stress (P3), called maximum compressive stress if negative, compresses them; the dilatational stress (DS) changes their volume, expansion if positive or shrinkage if negative; and the von Mises stress (vMS) distorts them. These mechanical stimuli cause biological reactions of the cells,[2] but the mechanism is not clear. To understand the mechanism, it is critical to quantify the ME changes.

Canine retraction is common and usually treated with one- or two-step methods.[3–6] The two-step process involves initial canine retraction to create space to alleviate incisor crowding followed by third-order correction.[3] A one-step approach is en-masse space closure with a rectangular archwire.[3,5,6] A frictionless T-loop is appropriate for canine retraction.[1] A power-arm (P-A) with a line of force through the center of resistance (C_{res}) of the canine is usually preferable for sliding wire mechanics.[6,7] The P-A can be attached to the canine bracket or to the archwire (AW) mesial to the canine (Figure 1).[2,8] Comparative effects of the varying appliances on initial displacement, stresses, and the overall ME are unknown.

The purpose of this study was to quantify the ME changes on the mandibular canine when the tooth is retracted using the three different orthodontic methods. The objectives were to evaluate how the methods affect ME changes and to determine the impact on clinical outcomes.

MATERIALS AND METHODS

For modeling purposes, a symmetric lower arch was defined bilaterally as L1-6 from central incisor to first molar with the first premolar (L4) extracted. The anterior segment was retracted with the one- or two-step method.

A three-dimensional (3D) finite element (FE) model was created based on dental and alveolar morphology of an anonymous adult patient who was imaged with cone-beam computed tomography. The study was approved by the Indiana University institutional review board (study 1011003026R005). MIMICS 16 image-processing software (Materialise, Leuven, Belgium) was used to construct a 3D model of the teeth and supporting tissues. The roots of the teeth were connected to a 0.2-mm layer of PDL that was supported by a 0.2-mm thickness of cortical bone. The stainless steel brackets on five mandibular teeth (L1, L2, L3, L5, and L6) had a slot size of 0.5588-mm (0.022-in). AWs and power-arms (P-As) were made from rectangular stainless steel (0.4064 $\times$ 0.5588 mm or 0.016 $\times$ 0.022 in). The Young modulus (E) and Poisson ratio for all materials (Table 1) were taken from previous studies.[1,9] Three types of mechanics were studied: (1) L3 retraction with a TL, (2) en-masse retraction with a P-A on the L3 bracket (PAB), and (3) P-A on the AW mesial to L3 (PAW). The loading by the specially designed TL was obtained experimentally[1] and used in previous FE analyses.[8,10]

The retraction force for each mechanism was 125 cN.[8,10,11] TL design was based on the patient's cone-beam computed tomography scan and validated experimentally. Gable bends were made to minimize rotation and tipping (Figure 1). The details were published previously.[1] P-A length was 8.323 mm apical to the plane of the AW, which allowed the retraction force to be at the same level as the L3 C_{res}.[12] The P-A were either attached to the L3 bracket (PAB) or to the AW midway between L2 and L3 (PAW) (Figure 1). Due to symmetry to the sagittal plane, only half of the dentition was modeled. Constrained surfaces were the central sagittal plane (symmetry), and the frontal plane distal to L6 (A in each diagram).[8] Surfaces A were fully constrained. The anterior surfaces, G for TL, as well as B and C for PAB and PAW, were constrained only in the direction perpendicular to the labial surface because this plane was the plane of symmetry.[8]

Tetrahedra elements were used to model the tissues and appliances. The interface of a bracket holding the AW was modeled using contact elements allowing relative motion between the wire and the brackets, except for the bracket-archwire interfaces of the anterior teeth for PAB and PAW where no relative displacement was allowed because they were typically bonded clinically. The interfaces were constrained as no separation and considered frictionless, reflecting lubrication by saliva. The details of the modeled interfaces were described previously.[8]

The element size for the model was determined through a convergence test.[8] Variation of displacement was less than 0.5% when the element number exceeded 125,196, so the final element numbers for the three models were 208,708 elements for TL, 576,144 for PAB, and 576,856 for PAW.

MIMICS 16 was used to segment tooth roots from the supporting bone. Creo Parametric 2.0 (PTC, Boston, MA) and ANSYS workbench 17.1 (ANSYS, Canonsburg, PA) were used to create the FE model

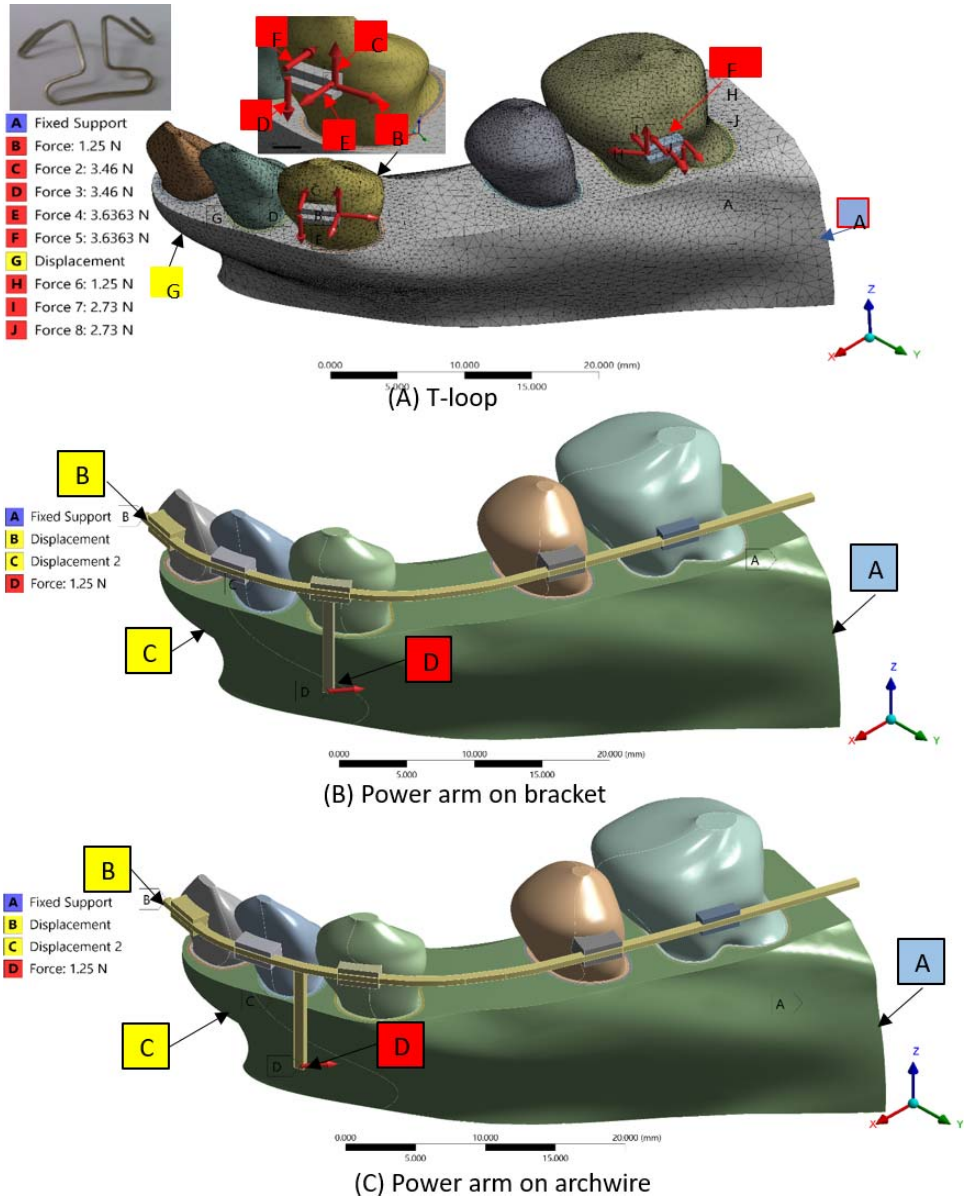

Figure 1. FE models are shown for three appliances to retract the lower anterior segments into L4 extraction sites. (A) The L3 and L6 abutments are shown for a previously published TL retraction model.[1] The equivalent forces (B through F) resulting from TL activation are shown as the basis to construct the other two models depicted in Figures 1B and C. The load system is a retraction force of 125 cN plus anti-tip and anti-rotation moments designed to translate the L3 distally. Constraints are imposed on the surfaces of A and G. The retraction force closely approximates the center of C_{res} for L3. The parameters for the equal and opposite load on L6 (H through J) are shown, but only the retraction of the anterior segment is reported here. See text for details. (B) The model was constrained at the surface A, B, and C. P-A extending to the level of the C_{res} of the L3 is attached to the L3 bracket (PAB). The same retraction force of 125 cN (red arrow) was applied at the end of the P-A. (C) The model was constrained at the surface A, B, and C. P-A at the level of L3 C_{res} is attached to the AW mesial to L3 (PAW) and is loaded with the same retraction force (125 cN).

Table 1. Material Properties of the Models and the Sources

	Young Modulus	Poisson Ratio	Reference No.
Tooth	20,000 MPa	0.3	8
Periodontal ligament	0.47 MPa	0.45	11
Cortical bone	13,000 MPa	0.3	8
Cancellous bone	1,000 MPa	0.3	8
Archwire	193,000 MPa	0.31	ANSYS database
Bracket	193,000 MPa	0.31	ANSYS database

Table 2. Maximum and Minimum Values of the Stresses in the Anterior Teeth PDL and Displacements That Occurred on the Teeth From the Three Types of Appliances: PAB, PAW, and TL[a]

	PAB		PAW		TL	
Stress Type	Max	Min	Max	Min	Max	Min
vMS (KPa)	24.52	2.72E-02	32.21	0.32	8.25	7.52 E-4
P1 (KPa)	26.34	–25.13	60.17	–33.41	11.66	–12.1
P3 (KPa)	19.14	–32.3	43.23	–45.28	9.26	–15.1
DS (KPa)	21.6	–27.7	47.59	–37.51	10.08	–13.12
Displacement (μm)	6.52	0.38	11.48	1.01	2.34	0.16

[a] DS indicates dilational stress; Max, maximum; Min, minimum; PAB, en-masse space closure with the power-arm on the canine bracket; PAW, power-arm directly attached to the archwire mesial to the canine; TL, T-loop; vMS, von Mises stress.

and to calculate tooth displacements and the associated stresses in the PDL.

RESULTS

Maximum canine displacements for each appliance were 2.34 μm (TL), 6.52 μm (PAB), and 11.48 μm (PAW) (Table 2). All of the methods resulted in some distal movement of the canine crown, but the displacement patterns were distinctly different (Figure 2A through C). TL produced translation and slight distal tipping of L3 in the sagittal plane. The PAB method resulted in distal-in rotation, but the PAW markedly extruded and tipped the canine lingually.

Figure 3 shows the distribution of P1 in the PDL. Maximum levels were all in tension: 11.66 KPa, 26.34 KPa, and 60.17 KPa for TL, PAB, and PAW, respectively (Table 2). The locations and distributions for maximum PDL stresses for P1, P3, vMS, and DS were different in magnitude and distribution (Figure 3).

Figure 4 illustrates the distribution and magnitude of P3 in the PDL. Maximum compressive stresses were –15.19 KPa, –32.3 KPa, and –45.3 KPa for TL, PAB, and PAW, respectively (Table 2). The locations and distributions of the maximum were different in both magnitude and distribution for all three appliances.

Figure 5 shows results for vMS: 8.25 KPa, 24.52 KPa, and 32.21 KPa for TL, PAB, and PAW, respectively (Table 2). Similar to P1 and P3, the stress distributions were different.

Figure 6 shows the different ranges for maximum and minimum DS in the PDL: –13.12 to 10.08 KPa for TL, –27.70 to 21.60 KPa for PAB, and –37.51 to 47.59 KPa for PAW (Table 2). The stress distributions were significantly different.

DISCUSSION

To compare the effect of appliance design to the tooth movement response differentially, the same magnitude (125 cN) of activation force was used for all three appliances. Only the ME changes for the anterior segment (canines and incisors) are described here.

The FE models calculated the instantaneous displacement and PDL stress associated with the applied load (Figure 2). The displacement reflects the action of a unique 3D load system acting on each tooth. Despite an identical activating force (125 cN), canine displacement and PDL stress were remarkably different between appliances. The specially designed TL[1] retracted the canine in the sagittal plane as a near translation response because both tipping and rotation were controlled with the anti-tipping and anti-rotation moments.[1] As the L3s are retracted with a TL spring, the L1s and L2s are tipped distally due to the pull of the supracrestal fibers.[13] This is an uncontrolled tip of the incisors because the supracrestal fiber force is applied coronal to the C_{res}.[12,14]

En-masse retraction with a rectangular AW attempts to maintain an ideal axial inclination for all teeth in the arch as the space is closed. An identical retraction force was applied at two locations (Figure 1). The line of force relative to the C_{res} and the central axis of the canine are critical considerations for determining the pattern of displacement (Figure 2A through C).[6,7,12] Force applied to a bracket on the buccal surface of the crown results in moments in the sagittal and occlusal planes. P-As on brackets are designed to apply a retraction force at the level of the C_{res} in the plane of tooth movement to achieve translation rather than tipping.[4] However, a line of force through the bracket is eccentric to the central axis of the canine so it produces a distal-in moment in the occlusal plane (Figure 2B).[14] Attaching the P-A to the AW mesial to L3 controls the undesirable moment in the occlusal plane, but distortion of the AW occurs, due to a lever-arm effect, that produces extrusion and a crown lingual moment of L3 (Figure 2C). Despite the same retraction force, each of the three appliances produced a distinctly different effect on the canines and incisors (Figure 2A through C).

There are many options for closing lower premolar extraction space(s). The initial displacement response (Figure 2A through C) is the primary indication for a path of tooth movement that achieves a specific treatment strategy. The TL is designed to retract the canine within the sagittal plane of the buccal seg-

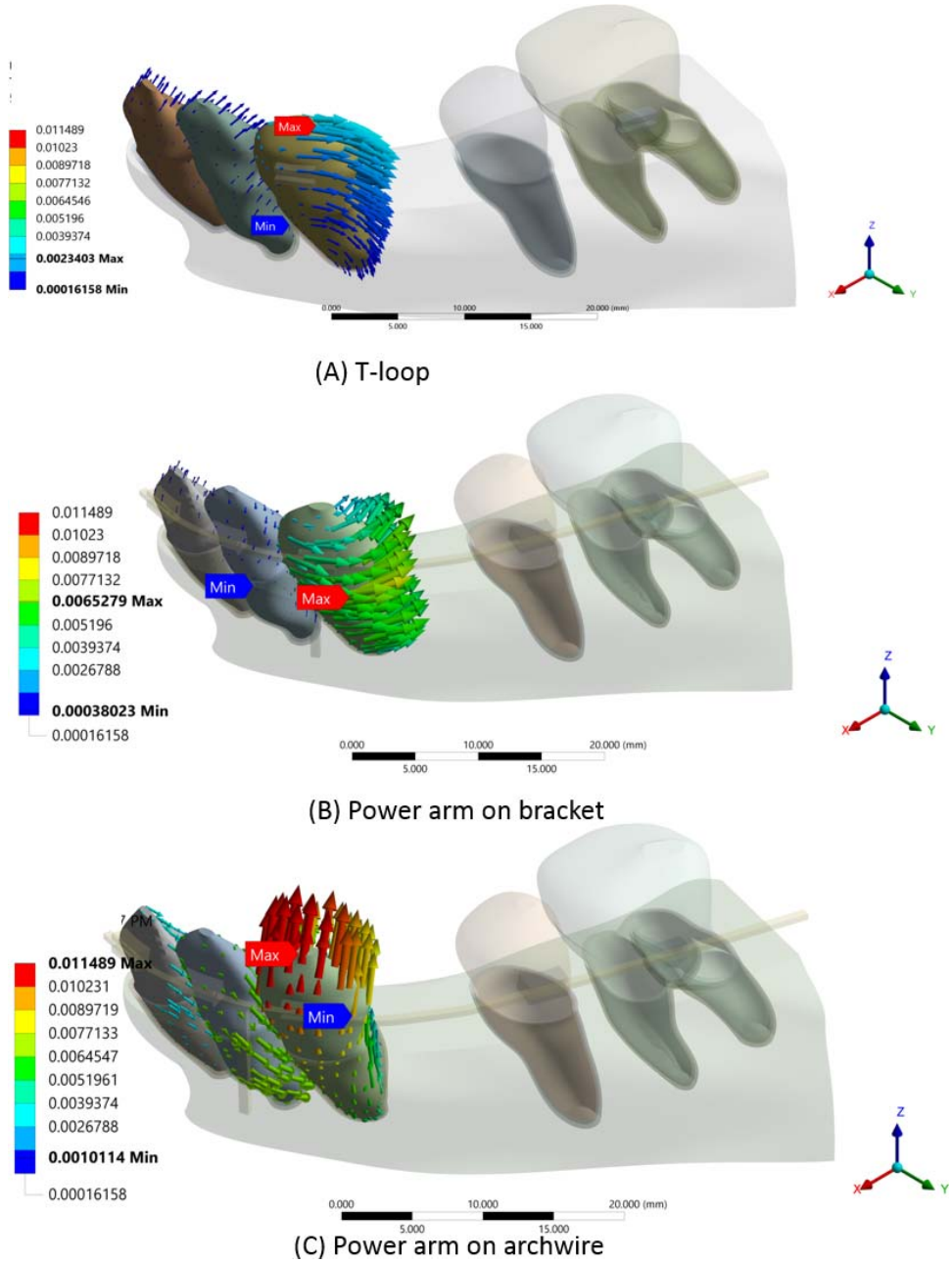

Figure 2. Comparison of tooth displacements and patterns are shown for the three models: (A) TL, (B) PAB, and (C) PAW. Both maximal (Max) and minimal (Min) principal stresses are illustrated. See text for details.

ment.[1,3–5] It is a relatively consistent appliance for translating canines, which is predictable clinically because it is a statically determinate system. On the other hand, en-masse sliding mechanics activated with a P-A is less predictable because it is a statically indeterminate system and the effect may vary depending on the position of the P-A (Figure 2B and C).

PDL Considerations

The differential displacements associated with each appliance (Figure 2A through C) are associated with specific patterns of PDL stresses defined as the P1, P3, vMS, and DS (Figures 3 through 6).[15] The orthodontic response to an applied load ultimately depends on the ME of PDL. Tooth movement depends on periodontal mechanotransduction to elicit bone modeling and remodeling within the PDL and the adjacent alveolar process supporting the root of a tooth.[16]

PDL is a genetically defined tissue that serves as a precise mechanotransductor for eliciting adaptive bone modeling when a tooth is subjected to a continuous

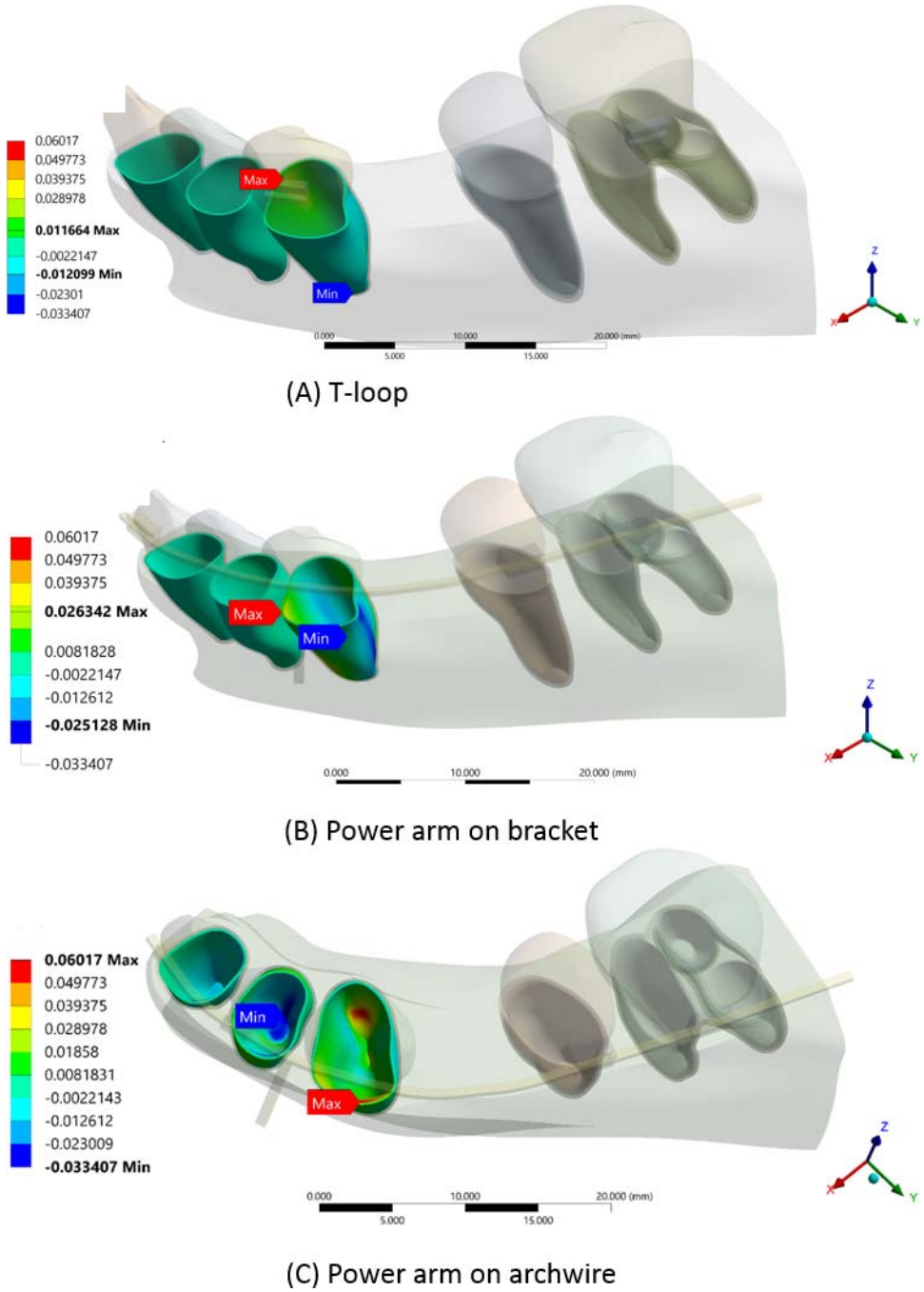

Figure 3. Maximum (Max) and minimum (Min) tensile stresses (first principal stress) in the PDL are shown for the three models: (A) TL, (B) PAB, and (C) PAW. Positive stress is tensile and negative stress is in compression. See text for details.

load.[13,16] Small continuous loads readily displace the root of a tooth within the PDL space,[13,14,16,17] which results in change of PDL electrical potential, triggering bone modeling and remodeling.[13] Pressure necrosis occurs if P3 exceeds 8–10 kPa, which is only about half the pressure required to block capillary blood flow.[17]

The ME is evaluated with DS and vMS. Relative to the PDL, there is an important distinction between DS and vMS. Change in DS assesses the pressure on cells and the stimulus for mobility of ground substance. The latter flows out of areas with more negative DS and into areas with more positive DS. The vMS assesses element distortion with no volumetric change, that is, shear effect that is not related to the flow of cellular or tissue components. DS and vMS are unique to the point or element[2] and, thus, are the preferred parameters for the current study. This

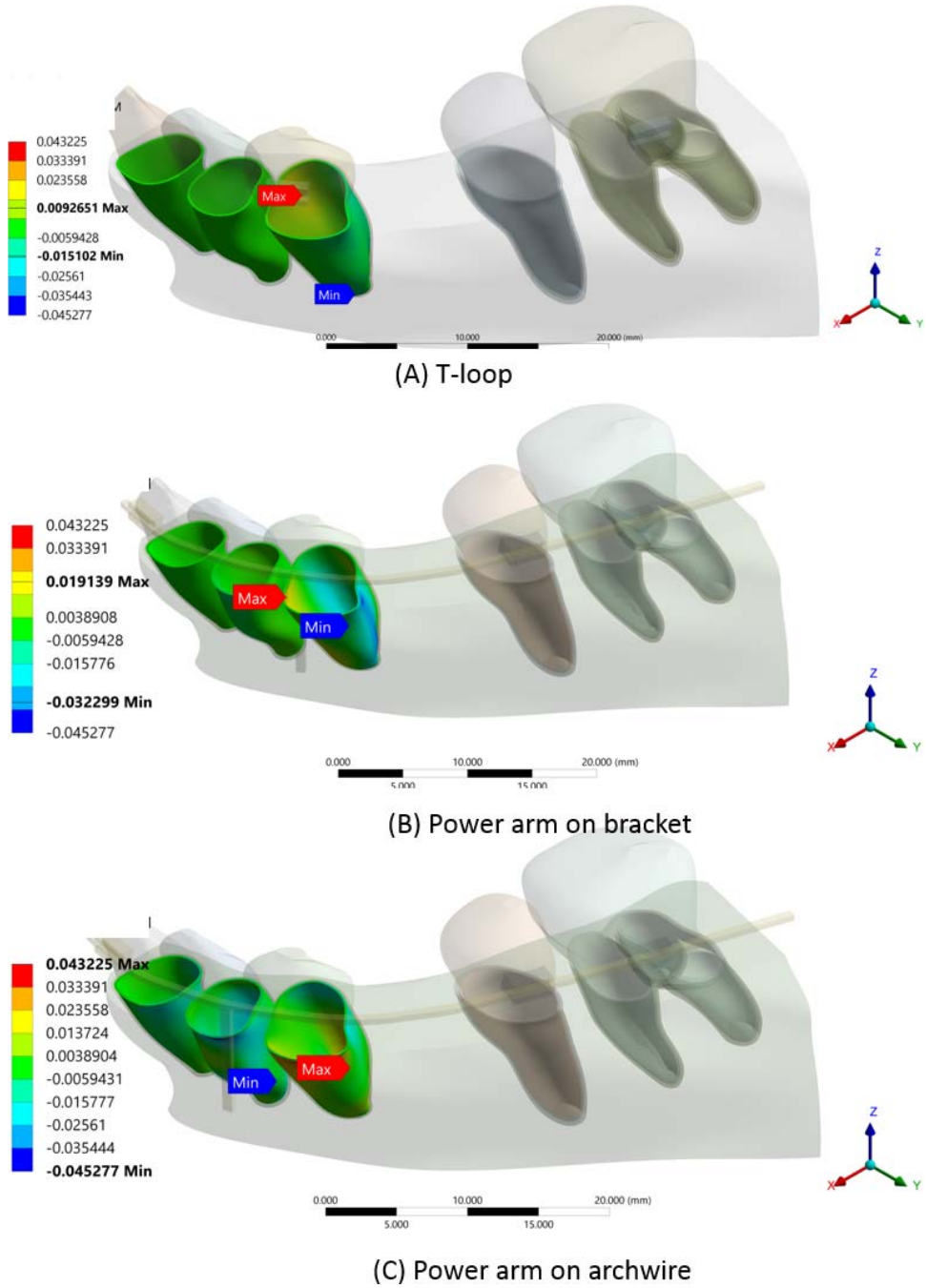

Figure 4. Comparison of the maximal (Max) and minimal (Min) third principal stress (P3) in the PDL is illustrated for the three models: (A) TL, (B) PAB, and (C) PAW. Positive stress is tensile and negative stress is in compression. See text for details.

approach is particularly useful for studying the mechanical conditions associated with initiation of the PDL response to different types of appliances.[18]

Within a mechanically defined window, stress levels determine the PDL biologic response.[19] There is a stress threshold effect (resistance number) for initiating tooth movement that varies according the type of load as well as the geometry of a tooth root relative to the alveolar process.[20] However, the therapeutic window is narrow because PDL undergoes necrosis if localized stress is excessive.[13,17,18] The threshold for PDL necrosis is P3 >8–10 kPa.[8,10,20] DS is an important parameter for selecting an appropriate orthodontic load.[21,22] Among the three methods, TL resulted in the lowest DS, which did not exceed the necrotic threshold in most locations. Compared with TL, PAB and PAW generated 2–4 times higher DS, so more PDL necrosis is expected. All stress invariants calculated were

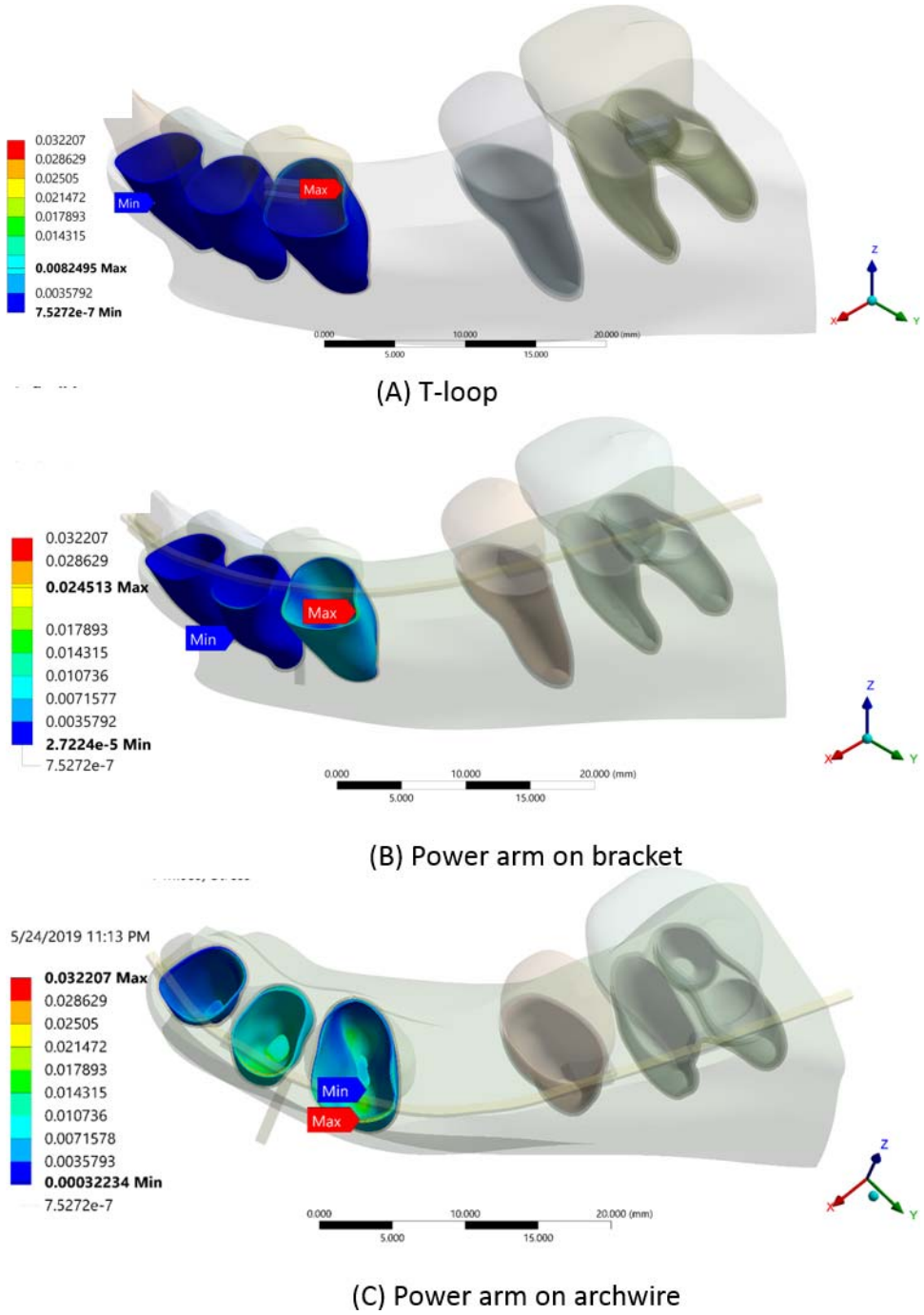

Figure 5. Comparison of the maximal (Max) and minimal (Min) vMs stress in the PDL is shown for the three models: (A) TL, (B) PAB, and (C) PAW.

significantly different among the three appliances (Figures 3 through 6). As the clinical response is clarified, calculating stress invariants will be critical for determining the optimal applied load for each orthodontic appliance.

The present research demonstrated that vastly different stress distributions can result from the same load applied to the three different appliances (Figures 2 through 6). Changes in the ME reflect the type of appliance, geometry, applied loading, and boundary conditions. The current results are difficult to compare to previously published reports because of different appliance design and loading conditions.[6,16,17] More consistent modeling protocols would enable compari-

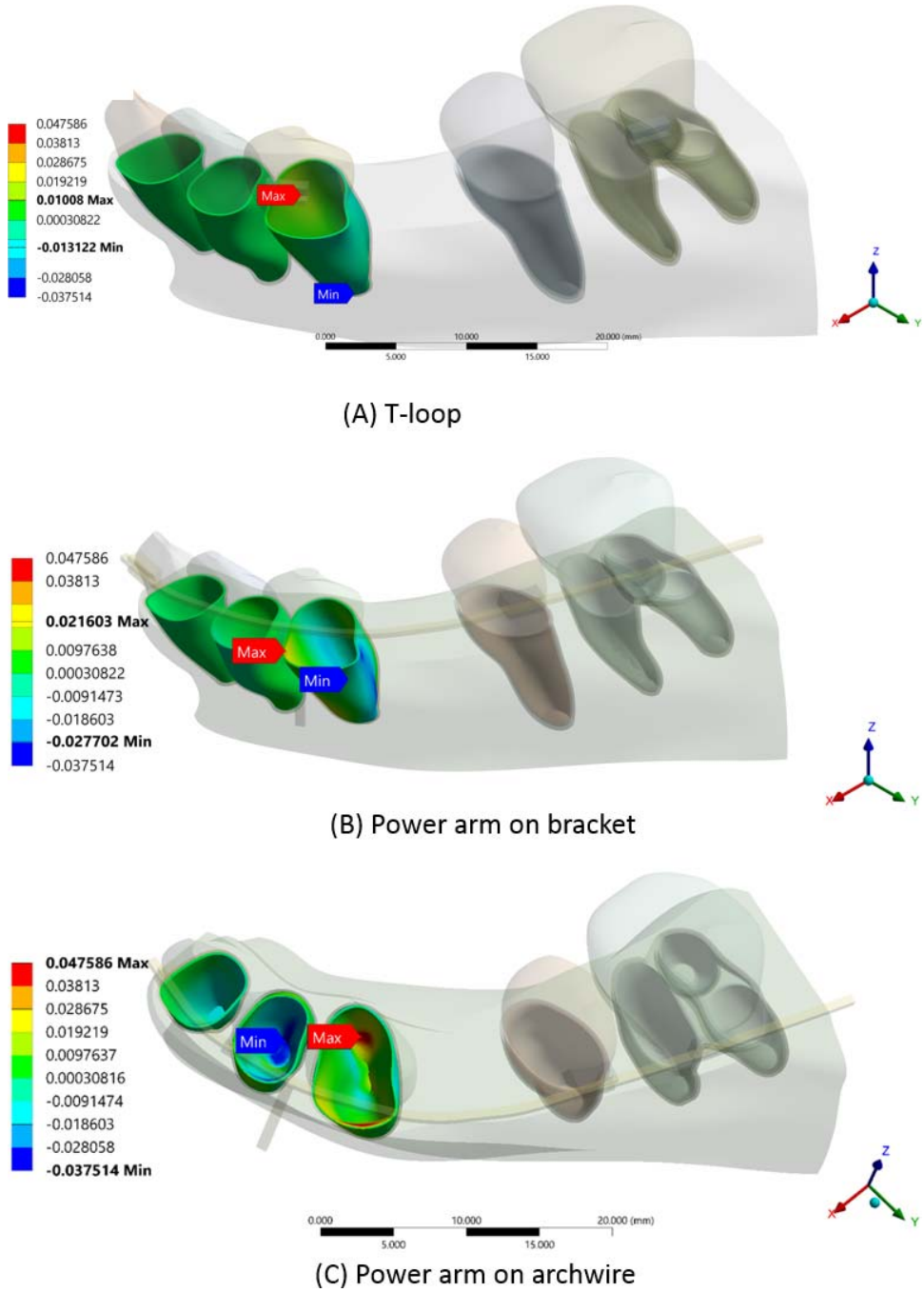

Figure 6. Comparison of the maximal (Max) and minimal (Min) dilatational stress in the PDL is shown for the three models: (A) TL, (B) PAB, and (C) PAW.

son, which would increase the understanding of effects from different appliances.

CONCLUSIONS

The conclusions drawn from analyzing the appliance configurations shown in this paper were the following:

- Tooth movement is appliance specific even when the same load is applied.
- A force through the plane of the C_{res} may produce undesirable side effects because of the 3D mechanical environment.
- A P-A attached to an AW may produce moments that distort the AW and move a tooth (teeth) in an undesirable direction.
- Compared with segmental TLs for canine retraction, delivering the force via a P-A results in elevated stresses in canine PDL.

REFERENCES

1. Xia Z, Chen J, Jiangc F, Li S, Viecilli RF, Liu SY. Load system of segmental T-loops for canine retraction. *Am J Orthod Dentofacial Orthop*. 2013;144:548–556.
2. Chetan S, Keluskar KM, Vasisht VN, Revankar S. En-masse retraction of the maxillary anterior teeth by applying force from four different levels—a finite element study. *J Clin Diagn Res.* 2014;8:ZC26–30.
3. Pervin S, Rolland S, Taylor G. En masse versus two-step retraction of the anterior segment. *Evid Based Dent*. 2018; 19:111–112.
4. Rizk MZ, Mohammed H, Ismael O, Bearn DR. Effectiveness of en masse versus two-step retraction: a systematic review and meta-analysis. *Prog Orthod*. 2018;18:41.
5. Schneider PP, Gandini Junior LG, Monini ADC, Pinto ADS, Kim KB. Comparison of anterior retraction and anchorage control between en masse retraction and two-step retraction: a randomized prospective clinical trial. *Angle Orthod*. 2019; 89:190–199.
6. Tominaga JY, Tanaka M, Koga Y, Gonzales C, Kobayashi M, Yoshida N. Optimal loading conditions for controlled movement of anterior teeth in sliding mechanics. *Angle Orthod*. 2009;79:1102–1107.
7. Ozaki H, Tominaga JY, Hamanaka R, et al. Biomechanical aspects of segmented arch mechanics combined with power arm for controlled anterior tooth movement: a three-dimensional finite element study. *J Dent Biomech*. 2015;6: 1758736014566337.
8. Liu Y, Jiang F, Chen J. Can interfaces at bracket-wire and between teeth in multi-teeth finite element model be simplified? *Int J Numer Method Biomed Eng.* 2019;35(3): e3169.
9. Qian H, Chen J, Katona TR. The influence of PDL principal fibers in a 3-dimensional analysis of orthodontic tooth movement. *Am J Orthod Dentofacial Orthop*. 2001;120: 272–279.
10. Jiang F, Xia Z, Li S, Eckert G, Chen J. Mechanical environment change in root, periodontal ligament, and alveolar bone in response to two canine retraction treatment strategies. *Orthod Craniofac Res*. 2015;18(suppl 1):29–38.
11. Xia ZY, Jiang FF, Chen J. Estimation of periodontal ligament's equivalent mechanical parameters for finite element modeling. *Am J Orthod Dentofacial Orthop*. 2013; 143:486–491.
12. Jiang F, Kula K, Chen J. Estimating the location of the center of resistance of canines. *Angle Orthod*. 2016;86:365–371.
13. Roberts WE. Bone physiology, metabolism and biomechanics in orthodontic practice. In: Graber LW, Vanarsdall RL Jr, Vig KWL, eds. *Orthodontics: Current Principles and Techniques*. 4th edition. St Louis, MO: Elsevier Mosby; 2012: 287–343.
14. Burstone CJ. Application of bioengineering to clinical orthodontics. In: Graber LW, Vanarsdall RL Jr, Vig KWL, eds. *Orthodontics: Current Principles and Techniques*. 4th edition. St Louis, MO: Elsevier Mosby; 2012:345–380.
15. Ansel C, Ugural SKF. *Advanced Strength and Applied Elasticity*. Upper Saddle River, NJ: Prentice Hall PTR; 2003.
16. Viecilli RF, Katona TR, Chen J, Hartsfield JK Jr, Roberts WE. Orthodontic mechanotransduction and the role of the P2X7 receptor. *Am J Orthod Dentofacial Orthop.* 2009;135: 694 e691–616; discussion Volume 135, Issue 6, P694.E1-694.E16, June 01, 2009.
17. Viecilli RF, Kar-Kuri MH, Varriale J, Budiman A, Janal M. Effects of initial stresses and time on orthodontic external root resorption. *J Dent Res*. 2013;92:346–351.
18. Barbagallo LJ, Jones AS, Petocz P, Darendeliler MA. Physical properties of root cementum: part 10. Comparison of the effects of invisible removable thermoplastic appliances with light and heavy orthodontic forces on premolar cementum. A microcomputed-tomography study. *Am J Orthod Dentofacial Orthop.* 2008;133:218–227.
19. Uhlir R, Mayo V, Lin PH, et al. Biomechanical characterization of the periodontal ligament: orthodontic tooth movement. *Angle Orthod*. 2017;87:183–192.
20. Viecilli RF, Burstone CJ. Ideal orthodontic alignment load relationships based on periodontal ligament stress. *Orthod Craniofac Res*. 2015;18(suppl 1):180–186.
21. Li S, Xia Z, Liu SS, Eckert G, Chen J. Three-dimensional canine displacement patterns in response to translation and controlled tipping retraction strategies. *Angle Orthod*. 2015; 85:18–25.
22. Song JW, Lim JK, Lee KJ, Sung SJ, Chun YS, Mo SS. Finite element analysis of maxillary incisor displacement during en-masse retraction according to orthodontic mini-implant position. *Korean J Orthod*. 2016;46:242–252.